

DOI: <https://doi.org/10.24297/ijct.v22i.9327>**Experimental Endoscope Rotitome-G: A pixel-by-pixel erasure microsurgical endoscopic sarcotome for resection of soft tissue tumours in closed body cavities**

Harjeet Singh Gandhi, MD, FRCS, FRCSC, MSc (Biomed Eng.)

Orthopaedic surgeon, Clinical assistant, Hamilton Health Sciences, Hamilton, Ontario, Canada

harjeetg52@yahoo.co.uk**Abstract**

Background: The procedure of minimal access to the brain through the nose is an ancient practice. However, endoscopic entry via a burr hole has recently gained significant traction in the practice of neurosurgery. High-resolution endoscopic images are possible with limited admittance of accessory tools and instruments. Although brain tissue can be removed easily with a suction device, but it will be uncontrolled 'excision'. The Rotitome-G is a precision micro-endoscopic target access surgical instrument. It has several accessories for intraoperative assessment and precise removal of the soft tissue lesions pixel-by-pixel within a closed body cavity through a single portal.

Objective: This preliminary theoretical research study on Rotitome-G is transition to experimental cadaveric and clinical studies. It describes the construction and mechanics of this newly conceptualized robot-assisted microsurgical endoscope. The design includes precise excision at the pixel and microscopic level and removes tissue debris under computer-aided navigation and direct instrument vision. Currently, the primary objective is to interest both the neurosurgeons and biomedical engineers, hence its contents are diverse resulting in an extended text.

Methodology: The study provides the basics of computer vision techniques and neuronavigation to establish the function and application of the Rotitome-G. The structure and kinematics of the animalcule Rotifer have been considered followed by the construction of Rotitome-G. For a better understanding of intracranial tumour excision, the article examines the role of intra-operative imaging, biomechanics of brain tissue, and brain shift to better understand the principles of this newly conceived microsurgical instrument. The functional capabilities of the instrument have been putatively demonstrated by describing the excision of a glioblastoma.

Conclusion: It is expected that the key design of Rotitome-G would meet the goal of neurosurgical resection by excising maximum amount of pathological tissue. Direct microscopic resection will prevent damage to the eloquent areas to improve the prognosis by limiting neurological morbidity. Clinical validity of the Rotitome - G remains to be determined.

Keywords: Flexible micro-endoscope, Neuroendoscopy, Optoelectronic, Neuronavigation, Brain shift, Brain biomechanics, Glioblastoma, Brain tumours, Neurosurgery, Endoscopy

1.0 Background to the proposal of Rotifer sarcotome

The Rotitome-G is a flexible precision micro-endoscopic surgical instrument designed to mimic the anatomy and physiology of the head and corona of the rotifer animalcule. The most interesting feature within the structure of the corona or crown-shaped face of this micro-organism is an arrangement of the cilia around its oral cavity. The cilia beat in-tandem, one after the other, to give it the appearance of a rotating wheel, hence its name. This fascinating rotating mechanism is a key design feature of the Rotitome-G, to form its cutting tool. The cutting tool bites into soft tissue lesions and drives the cut fragments into the aperture of its aspirating channel, making it a sarcotome (soft tissue cutter). The ability to introduce Rotitome-G through a single small incision or an aperture to access target lesions within closed body cavities makes it a 'target access' surgical instrument.

1.1 Traditional and minimal open surgical access

The traditional surgical techniques are definite layer-by-layer direct anatomical access to an operative field. The length and curve of an incision are based on the site and extent of index surgical activity. It depends either on the size and depth of the pathology or the size of the repair and replacement implant for reconstruction. Such measured access demands meticulous dissection, where each anatomical layer is divided and the next level is exposed without causing unnecessary crushing, tearing, excessive use of cautery, and wayward cuts, to limit damage to the surrounding healthy tissues. The concept of minimal access surgery was introduced to



limit the length of incisions, reduce collateral tissue damage, and better cosmetic healing. It possibly reduces surgical wound infection compared to wider exposure of the deeper tissues for prolonged periods. The minimal access surgery has remained in routine practice wherever applicable.

1.2 Key-hole access endoscopes

What is often called 'button or key-hole surgery, came with the advent of numerous varieties of endoscopes, rigid and flexible (Fig. 1). This was followed by steerable leading ends to have a maximum view of internal surfaces of the hollow organs and tubular structures, and excision of diseased organs. All endoscopes are either constructed of the light-conducting columnar lens in a rigid endoscope, or a bundle of flexible optical fibres aided with lenses and high definition charged coupled device (CCD) cameras. Kenji Takagi used a 7.3mm cystoscope for knee arthroscopy in 1918(Ainger & Gillquist, n.d.). In 1910, L'Espinase did fulguration of choroid plexus with hydrocephalus using a cystoscope and in 1935 Scarff reported neuroendoscopic procedure on third ventricle using an advanced scope with a cautery electrode and an irrigation system to distend and lavage the ventricle(K. W. Li et al., 2005; Shim et al., 2017).



A.



B.



C.

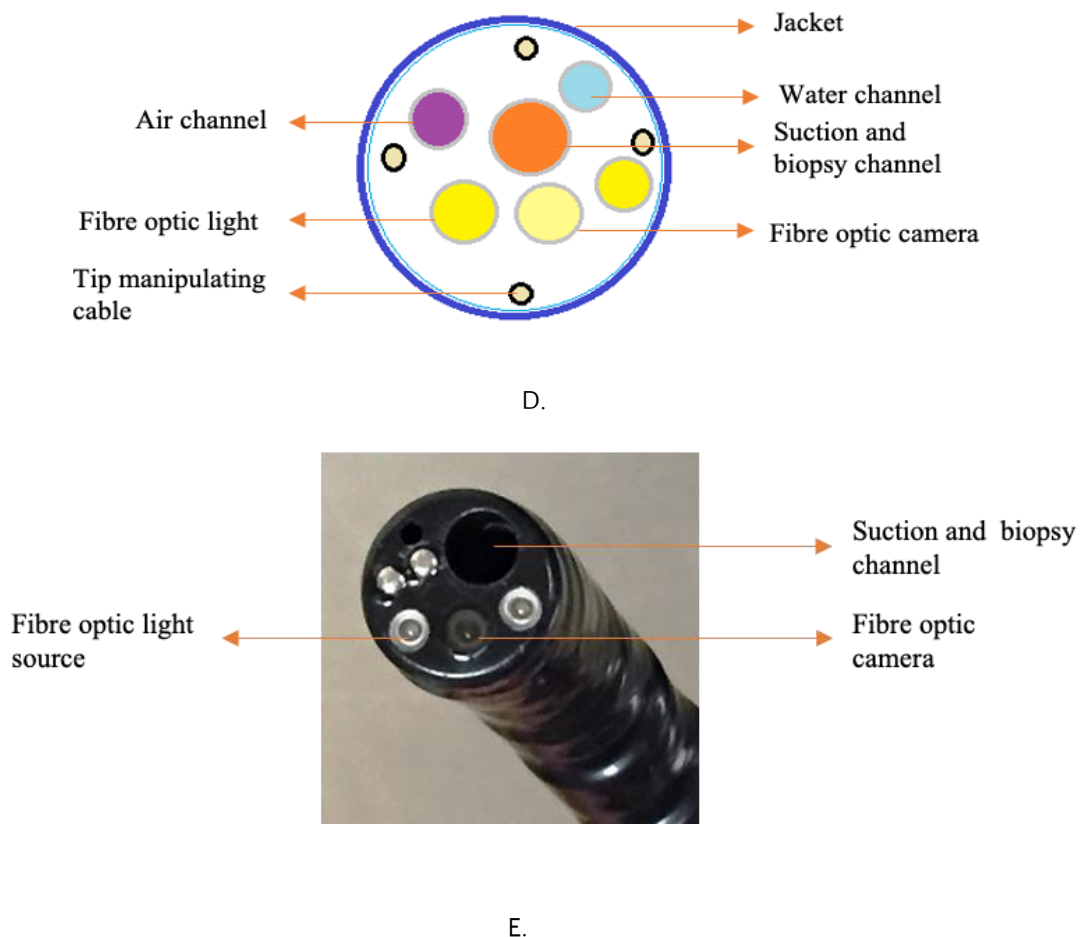


Figure 1. A. and B. A set of rigid 4mm knee endoscope, trocar, cannula, and camera; C. A flexible gastroscopium; D. A line drawing showing accessories at the leading face end of a gastroscopium; E. The steerable flexible end.

Most of the flexible endoscopes allow the insertion of other instruments to cut, cauterize and take tissue biopsies through the same unit. Making more than one portal is common to introduce assistive devices to pass sutures and larger cutting tools to remove pathological tissues in most surgical procedures within body cavities with rigid endoscopes. However, there are body cavities where it may not be feasible to make a second portal due to important anatomical structures in the vicinity that may come to harm moderating the overall outcome of the surgical procedure.

The term '*target access surgery*' is applied to endoscopic surgery performed through a single aperture or a burr-hole to access the cranial cavity under image guidance with the assistance of navigation tools to target specific anatomy of the brain. Unlike traditional key-hole endoscopic surgery, the target access surgical technique does not require a separate accessory portal for introducing cutting instruments to excise a pathological lesion. The robot-assisted target access surgery helps to overcome the inadequacies of hand-eye coordination and much-needed obligatory dexterous surgical skills for an open access surgery.

1.3 Intra-operative image-guided surgery

Only a few endoscopic procedures demand routine use of intra-operative image guidance to confirm the status of the endoscope in relation to the index pathology for satisfactory completion of the pre-operative surgical goals. Among all the surgical branches, the highest demand for intra-operative radiographic imaging with projection C-arm image intensifier is in orthopaedic and trauma surgery. With the arrival of navigation-

based surgery, the role of computed tomography (CT) is taking over some of the imaging requirements. In this race magnetic resonance imaging (MRI) is not far behind and has already started to change the architecture of the operating theatres in many hospitals around the world (Kacher et al., 2014). MRI is preferred during neurosurgery imaging and primary pre-operative diagnosis of the brain tumours because it is a non-ionizing radiation modality providing detailed expression of intracranial structures, brain topography and high definition of intra-cerebral tissues. In addition to T₁ and T₂ weighted images with tissue enhancing contrast, MRI has multimodal ability to acquire functional MRI (fMRI) and diffusion tensor imaging (DTI) to reveal the anatomy of motor and sensory tracts in the cerebral cortex, making it easy to identify and protect eloquent areas of the brain.

The application of ultrasound imaging within human body cavities as an endoscopic assistive device during surgery is now greatly refined. The improved ultrasound-guided imaging has been made possible due to the manufacturing of silicon-based capacitive micro-machined ultrasonic transducer technology for wider applications (Khuri-Yakub & Oralkan, 2011; Wygant et al., 2008). The capacitive ultrasonic transducer technology can deliver real-time 3D imaging for endoscopic surgery and other minimal access interventions.

1.4 Role of computer vision

The application of computer navigation tools to target surgical anatomy is dependent upon image segmentation and registration techniques, which are widely practiced for image processing and analysis. The process of image segmentation isolates finite anatomy to define the region of interest. Registration is correspondence between images obtained with the same or different modalities to transform the geometry of pre-operative and intra-operative images within the identical reference frame. The segmentation of a brain tumour at preoperative workup is imperative to acquire qualitative and quantitative metrics. Image segmentation of a significantly sized invasive tumour is not an easy task and it becomes even more difficult to update the image data due to local and global deformation of the organ as the surgery proceeds. There are numerous traditional manual and semiautomatic interactive techniques such as Snakes, thresholding, and edge-detection based on image intensity (Gandhi, 2022a) which are inconsistent due to operator and observer variations. Currently, automatic Deep learning segmentation methods such as Convolutional Neural Networks, encoder-decoder U-Net, etc., have been shown to be more promising for segmentation and registration (Bhandari et al., 2020). Intra-operatively, a non-rigid registration technique is preferred to isolate tumour boundaries in 2D CT and MRI slices for correspondence between coordinates of image space and tumour anatomy in physical space (Pohl et al., 2007; Warfield et al., 2000). In conjunction with pre-operative MRI, intra-operative 3D ultrasound is used to refresh segmentation and registration to redefine the tumour margins and quantification of the adjacent cavitation during tumour resection (Carton et al., 2020).

1.5 Navigation system and tracking devices

After segmentation and registration, the next step is visualization and navigation of the lesion in the image space in correspondence to the patient physical space. The navigation tools are designed to locate and integrate the surgical instruments in the surgical field within the coordinates of the reference frame (Hata, 2014; Zhao & Jolesz, 2014). Mathematically, three-dimensional volumetric image coordinates and the patient's anatomical coordinates are aligned in three orthogonal axes. In conjunction with image guidance, the navigation increases accuracy and improves the extent of resection at the periphery of malignant tumours. After the initial set-up, the navigation system with each image-guided update helps to control the depth, surgical trajectory, and finer movements of instruments within the segmented anatomy. The process of navigation during surgery may be operated under fluoroscopy, CT, or MRI imaging modalities (Zhao & Jolesz, 2014). Currently, some systems can be operated without the need for imaging. In the case of imageless systems, pre-operative or intra-operative input 3D reconstructed images are transferred to the navigation software program. The surgeon chooses the fixed anatomical landmarks and places the markers that can be identified by the optical camera system. It is processed by a computer in conjunction with the prepared 3D reconstructed image to generate a virtual model of the segmented anatomy as well as the surgical tool/s in the physical space.

At present, there are more than a dozen surgical navigation systems available in the market with varying capabilities (Karkenny et al., 2019). Passive navigation is an interactive system, which allows surgeon input to guide the tools as the circumstances change during surgery. Whereas an active navigation system is designed for automatic execution of the pre-planned task. It prevents manual intervention by the surgeon to change already calculated trajectories. Imageless active navigation systems can be expensive as it requires one or more targeting 3D printed jigs. Both types of systems can be operated by merging with surgical robotic systems, to improve surgical accuracy.

Fundamentally, whatever the system, navigation neurosurgery is based on stereotactic principles, and tracking devices are part and parcel of all navigation systems(Hata, 2014). Navigational tracking is an interactive localization process to define the patient's coordinate system to track the position of instruments in the physical space, relative to the patient anatomy. In the case of percutaneous target access surgery, such as endoscopic intervention, it is possible to develop a safe trajectory for an operative view of sub-cortical surgical pathology in the brain. When done with the help of navigational sensors in conjunction with a robotic system it brings greater precision in positioning the instruments in the physical space of pathological anatomy in correspondence to the image space. A rigid scope can be tracked with optical sensors fixed in a patient's 3D physical coordinates, but to virtually represent a flexible endoscope in the image space requires an electromagnetic tracking method(Gergel et al., 2011; Jolesz et al., 1997). Currently, the two commonly used optical tracking devices are passive infrared light reflectors and active light-emitting diodes. These wireless trackers mounted on surgical instruments are picked-up by multiple video cameras arranged in a 3D triangular space. The information is transmitted to the workstation to calculate and indicate the precise position of the instrument. However, the optical trackers require a clear line of sight within a busy operating room environment. Therefore, the electromagnetic tracking system is preferred, which consists of a signal emitter and a receiver nearby in the non-sterile zone, with a focus on the mobile surgical instrument.

Generally, a small electromagnetic sensor is placed on the instrument handle or the leading end of a flexible surgical instrument. The electromagnetic tracking sensor has a three orthogonal coil magnetic field generator that generates magnetic flux(Yaniv et al., 2009). The relative intensity of the current generated by the three coils calculates both location and orientation of the tool in the 3D pulsed magnetic field of known geometrical space. Miniature sensor coils (solenoids) less than 0.5mm diameter and 8mm in length are now available (Aurora® Northern Digital Inc. and the 3D Guidance med SAFE TM, Ascension Technology Corp. Burlington, VT) for inclusion at the leading end of a flexible endoscope in the tumour space. A single sensor can detect 3-degree of freedom (DOF) of location and orientation, and optimally placed two sensors allow sensing 6-DOF. The visual display unit of the navigation system displays pre-operative images, which can be co-registered to update patient images for calibration of the sensors to track the surgical instruments. Unlike the optical system, electromagnetic sensors do not get interrupted by the line of sight, but large ferromagnetic objects too close to the operating area will cause distortion in the image space. It essentially means the need for non-ferrous titanium or polymer-carbon fibre composite instruments compatible with this type of tracking technology.

The use of intra-operative image guidance and the application of navigation technology are well recognized in neurosurgery. It has brought significant improvement in safe intervention and the outcome of intracranial tumours. With increasing acceptance and frequent use of navigation tools, the frameless stereotactic operative method is becoming the standard of care in many surgical specialties, particularly in the treatment of intracranial tumours. The stereotactic approach allows the surgeon to either physically as an operator or with the assistance of a robotic arm move the surgical instruments and an endoscope within the sterile 3D coordinates of the operating field through exact correspondence to the image space. Integration and co-registration of parametric multimodality MRI images with stereotactic navigation help orient surgeons to locate normal and pathological anatomy and their segmented geometry to perform safe and effective resections. High-resolution MRI displays tumour infiltration into the eloquent areas, deformation of the anatomy, and reactive oedema outside the segmented pathology are all well-recognized features of invasive gliomas(Pallud et al., 2010) Such changes with tumour infiltration limit direct open access difficult to delineate surgical margins and risk eloquent areas.

Intra-operative imaging updates the anatomy and navigation guide the surgeon to chase after the residual suspicious infiltrating malignant tissue as surgery progresses. It is to protect the eloquent brain areas and shift of its neighbouring anatomical structures towards emptied tumour space(Warfield et al., 2005). In addition, the navigation of the neuro-endoscope and assistive surgical instruments require an interdisciplinary operating room team consisting of an operating surgeon, radiologist, and computer vision expertise of a clinical biomechanical engineer to update segmentation and co-registration of pre-operative and intra-operative images(Wittek et al., 2007).

2.0 Anatomy and kinematics of rotifers

Rotifers are exquisite metazoans, 50-2000 micrometer in length(Trout et al., 2002; Wallace, 2002). In 1702,



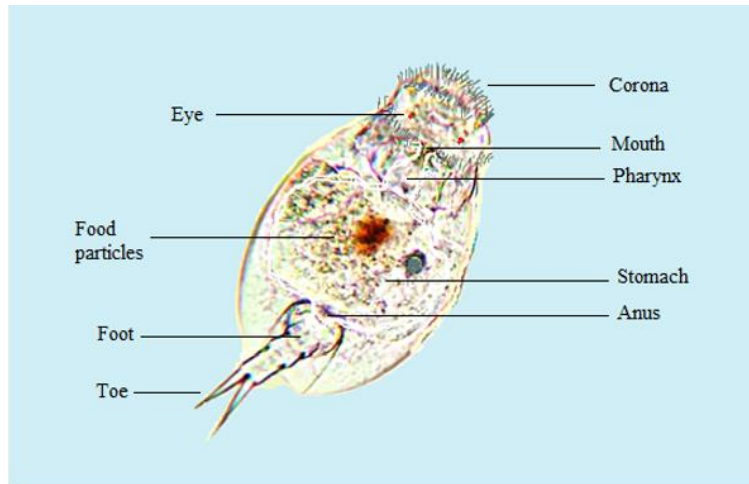


Figure 2. Elementary functional anatomy of a rotifer animalcule as related to the Rotitome-G, showing corona lined with cilia, eyes in red, mouth, stomach, and anus.

microscope pioneer, Van Leeuwenhoek, discovered rotifers when he rehydrated dry and apparently lifeless dust from a roof gutter with clean water in a glass tube. With his single-lens microscope, he noticed many animalcules becoming active within an hour “adhering to the glass, some creeping along with it and some swimming about”(Tunnacliffe & Lapinski, 2003).” These ‘rose coloured’ animalcules have a cylindrical body consisting of a head, trunk, and foot (Fig. 2) The head or corona has very distinctive concentrically arranged cilia in two rings, at its anterior end. The cilia beat at high frequency in a metachronous rhythmic and time-dependent in-tandem movements, giving an illusion of a rotating wheel, hence the name rotifer (L., rota + ferre, wheel bearers)(Wallace, 2002). An efficient and orderly beating of the cilia for locomotion also sweeps water and suspended particles towards the central oral cavity are masticated with chitinous plates that chops and push ingested matter inwards.

2.1 The concept of 'Rotitome-G

The imitation of regional anatomy of the corona and kinematics of oral structures of a rotifer is of interest in the engineering of the Rotitome-G sarcotome. This soft tissue cutter is adapted to resect diseased soft tissues pixel by pixel. The other structures of interest in the rotifer are organs of vision and sensory antennae to enhance the functional capability of the Rotitome-G. One of the two variations of the cutting end of the Rotitome-G sarcotome has circumferentially arranged filaments and the other is an iris-shutter cutting mechanism at the front end of the instrument. The sleeve around the cutting end carries assistive devices to assist pixelwise piecemeal resection of a sarcomatous lesion. As the operation of the Rotitome-G has been exemplified here by demonstrating resection of an intracranial glioblastoma, therefore it becomes necessary to understand the biomechanics of the brain, and surgical steps taken to maximize resection of a tumour.

3.0 Rotifer sarcotome - Rotitome-G

The Rotitome-G (Fig. 3 and 4) is a combination of a forward cutting high-speed rotary microtome and high-resolution micro-endoscope, fitted with a light-emitting diode (LED), infrared high inductance transducer, and monofilament monopole nerve stimulator, with the option of a capacitive ultrasonic micro-transducer. These devices embedded in the leading end of the instrument are combined to optimally mimic the anatomy and the physiology of the rotifer's head. The primary tool built in the head of the Rotitome-G is one of the variations of rotary microtome, while the other devices are to light-up sub-cellular vision, non-tactile infrared sensor to measure tissue density and focal electrical stimulation monofilament probe for eliciting function and definition of eloquent neural tissue. The goal is to accomplish micro-level resection of infiltrating rhizoid tissue extensions of a tumour safely and effectively within reach of the Rotitome-G. The micro-endoscopic devices

¹ Rotitome-G micro-endoscope and all accessory instruments integral to its functions and applications are intellectual properties of the author.

are already known to the community of optoelectronics to diagnose pre-cancerous and cancerous tissues after selectively staining with fluorescent dyes to image mitotic features of cell nuclei and quantify nuclear-cytoplasm ratio (Grant et al., 2019; Muldoon et al., 2007).

3.1 Construction and function of the Rotitome-G

The Rotitome-G is a flexible 4.5mm diameter fibre-optic instrument. The main components are (Fig. 3), 1. a centre axis end-on rotary cutting tool, 2. a fibre-optic micro-endoscope with a charged coupled device (CCD) camera, 3. light-emitting diodes (LED) to illuminate the field of view, 4. an infrared inductance non-tactile sensor, 5. a monofilament monopole nerve stimulator, and 6. option of the micro-ultrasonic transducer. The assistive devices to the central cutting tool arranged around the periphery of the end facet or face of the instrument are embedded in the wall of the outer housing analogous to the corona of the rotifer organism. In addition, within the enclosing sheath of the instrument are embedded electromagnetic sensors for navigating the leading end.

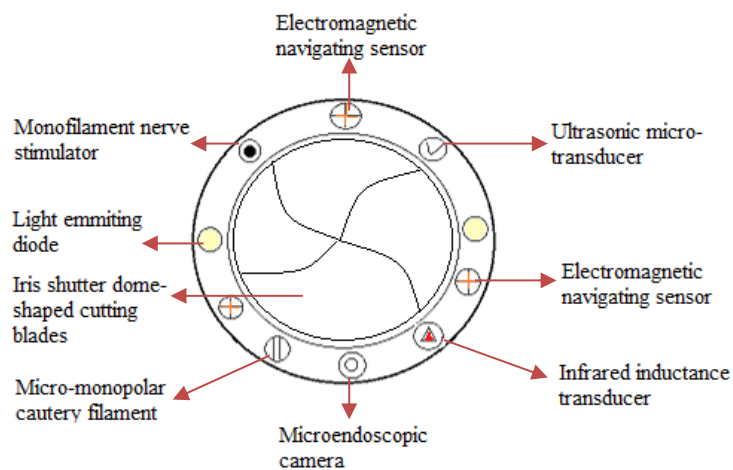


Figure 3. – Illustration showing retractable central iris shutter cutting blades of the Rotitome-G and assistive devices.

The centre axis occupied by the unique rotary cutting tool has a central bore or canal to aspirate the resected tumour tissue debris and blood, inject lavage fluid or even pass down a suitable micro-instrument such as a cauter, a micro ultrasound, or even a microlaser probe. One of the variations of the distal cutting tool is a high-speed rotary fixed-level multiple filaments arranged circumferentially around the aperture of the central aspirating canal (Fig. 5). These filaments are designed to make rotiferous movements to cut the tumour tissue, and simultaneously aspirate the resected tissue debris to an external receptacle for collection. The diameter of the cutting end and length of these filaments is to remove only tissue equivalent to the size of one or a few pixels in the representative image plane with similar depth. The other variation is a retractable cutting tool with a helical motion to move in and out of the peripheral housing cylinder to a definite depth of 1-2 pixels into the tissue for resection. The end-on face of this variation has a dome-shaped cutting surface consisting of an iris-shutter like the shutter mechanism of a classic photographic camera. The shutter design has three to four micro shutter blades with a positive rake angle on the deep surface in the direction of its rotation to bite and deposit the bolus of cut tissue into the axial aspirating bore as it retracts into the housing cylinder like the swallowing action. The impelling action of the cutting tools directing the debris into the axial bore of the torque shaft helps to keep the tumour space clean to provide a better view of the resected surface of the tumour tissue. The iris-shutter elements are made of hard-wear-resistant material. The objective of conferring the helical retraction mechanism is to drive in and out the cutting tool gradually rather than push and pull it out that may cause rupture of more tissue than desired by the operator and inadvertent bleeding.

The pixel-eating action of the cutting tool is actuated with a handheld cursor locator device, such as a computer mouse, in the image space of the visual display unit (VDU) screen. The protrusion and retraction, and tissue nipping action are actuated during the press and release of actuating a button on the handheld device that drives the cursor. The choice of iris-shutter cutting variation is most preferred at the edge pixels, to resect infiltrating tissues close to the eloquent tissue to take pixel by pixel bites after reviewing the microscopic structure of the tissues ready for resection. At the same time, taking full advantage of monopole nerve stimulating monofilament and non-tactile sensor to elucidate density of the tissues.

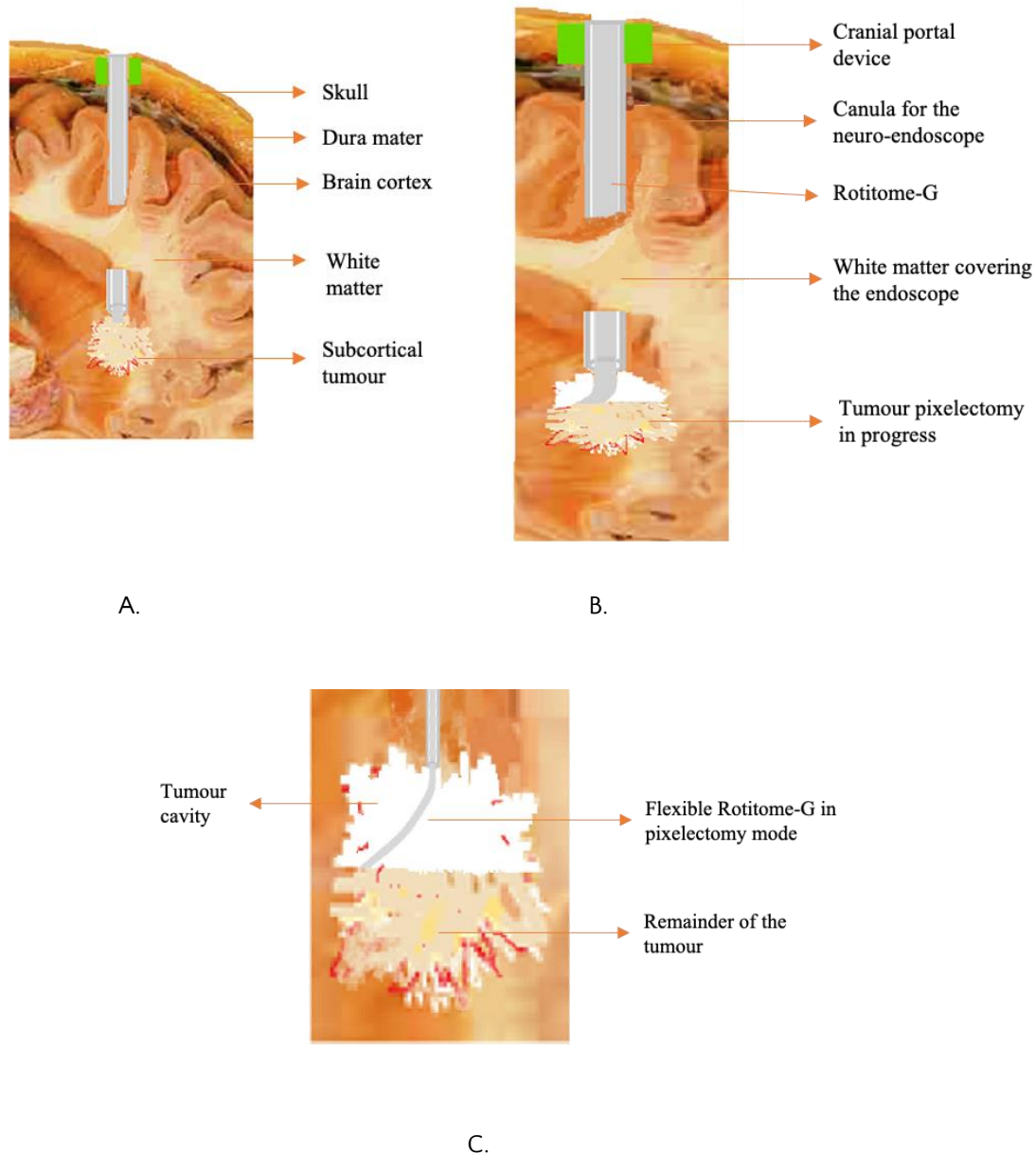


Figure 4. – Illustration A. Showing a section of the brain and a line drawing of Rotitome-G flexible endoscope placement to approach a subcortical tumour. B. An expanded segmental view of to show the action of the flexible cutting end in the grazing mode. C. A raster image depicting the appearance at pixel level during pixellectomy of the tumour. (Section of the brain adapted and modified from Rohen, Yokochi, Luten-Drecol, Color atlas of anatomy, 7th ed., 2011, Lippincott Williams & Wilkins.)

The unique cutting tool assembly in the centre axis rotates relative to the outer housing cylinder of the flexible Rotitome-G instrument (Fig. 4 and 5). The central assembly of the flexible torque shaft operates with a non-touch electro-magnetic high-speed rotating mechanism within the outer housing of the instrument. The rotary

cutting head coupled to the torque shaft is kept axially stable within the outer housing distally and proximally by snap-on ring bushings made of the highly wear-resistant coated material. Within the flexible housing sheath, the head of the cutting tool is coupled to the torque shaft with a universal articulation. The universal joint design gives fibre-optic device 360-degree multi-plane arc tracing capability with the maintenance of aspirating channel patency. The steerable head with sweeping and grazing ability increases tissue resection

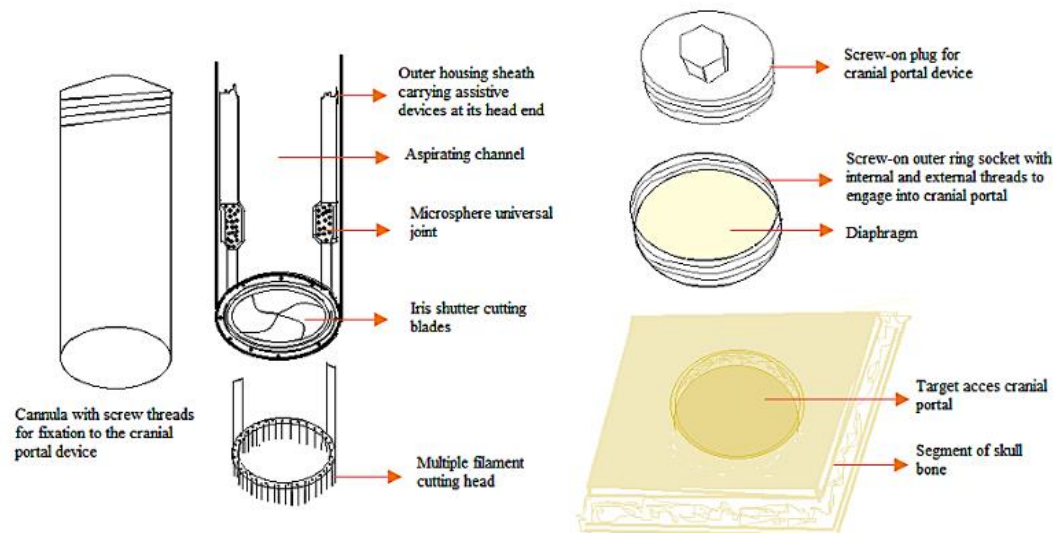


Figure – 5 Illustration showing prototype design features of the Rotitome-G and cranial portal device to engage the Rotitome-G to the craniotomy site

under direct instrument vision in hard-to-access areas and retro-vision of the tumour space with the help of incorporated high-resolution micro-endoscope. As the forward resection proceeds, the crane-neck retro-flexion mobility of the grazing action of the cutting head at the universal joint can capture in-plane tissue and ceiling pixels of the tumour space. Steering, grazing, and sweeping action of the cutting tools can be automatic or manual for controlled tissue resection under direct visualization of the tumour boundary tissues and edge pixels in the image space. There is provision for the interactive control mechanism to manually steer cutting tool end independent of motorized torque shaft action as part of the same central assembly. Automatic control may be performed by open-loop operator entered settings and activated by a switch or in-built feedback mechanism to control the action of the cutting tool.

The assembly of the rotating mechanism can be inside or outside the sterile operating field with switches on the handheld unit for manual operation or adapted to a robotic arm for automatic function. There is no motion of the fixed sheath inserted at the time of initial operative set-up through the target access portal and for placement the Rotitome-G to traverse craniotomy and the cerebral parenchyma. The sheath to access the sub-cortical tumour remains motionless, fixed to the craniotomy burr-hole site with a screw-on watertight adaptor for the rest of the procedure.

The camera and the number of optical fibres in the bundle carrying the light determine the quality of the images and field-of-view. The LED to illuminate the field-of-view and micro-endoscope camera each has a separate bundle of the optimal number of optical fibres to collect sub-cellular level images. There are single optic fibre imaging modalities, but for the delivery of high-quality images, it is preferable to have enough optic fibres transferring images from a 10 megapixels CCD camera (Grant et al., 2019). The images are magnified by intervening optical lenses and filters for display on a VDU. The presence of corneal lens of the micro-CCD camera on the leading end provides the wide-angle microscopic vision to differentiate eloquent areas, preferably segmented from the tumour tissue during pixel-by-pixel cutting of infiltrating rhizoid tissues. The micro-endoscope has a very short focal length from direct contact with the tissues to a few millimeters. The obtained images may be segmented based on an intensity histogram to define the mitotic nuclei to increase

the probability of excluding eloquent tissues. In case a larger field-of-view is required mosaic-video facility may be included (Bedard et al., 2012).

A transducer is a device that produces usable output in response to a specific measurement (Instrument Society of America, ANSI MC 1, 1975). Transducers employ one or more transduction (transfer or convert one form of energy to another) mechanisms to generate an electrical output signal. There are biophysical-based optical sensors for intracranial pressure measurements and cancer tissue detection using laser and other fibre-optic probes. The fibre-optic devices have the potential to be miniaturized, made biocompatible and applicable for infrared far and near wavelength, fast being a light, and safe being non-tactile (Coté et al., 2003). An infrared inductance transducer can convert a physical quantity into measurable electrical quantity output. Alternatively, an acoustic sensor like a micro-ultrasound probe based on a piezoelectric mechanism may be included for tissue recognition. The kind built into the Rotitome-G micro-endoscope is an optical infrared beam deformation sensor to differentiate density between normal and tumour tissue.

Direct cortical stimulation is another well-established intraoperative technique for stimulating surface grey matter and subcortical white matter to assist with localization of the eloquent areas (pre-central motor cortex, descending motor tracts, speech areas, and brain stem) to prevent loss of vital neurological function post-operatively (De Witt Hamer et al., 2012). The low-frequency continuous stimulation is commonly used in awake patients and the delivery of high-frequency pulses makes it possible to stimulate the motor cortex in anaesthetized patients (M. Taniguchi et al., 1993). Unlike the bipolar surface probe monopole probe send current radially to cover greater brain tissue. It locates and maps tissues much farther away from the site of surgery to provide advanced warning to the surgeon. The Rotitome-G has monopole nerve stimulation filament on its face reach out into the brain tissues as it advances to take the next bite on the tumour tissue. The monopole filament can continuously monitor the function of the neural tissue before the cutting tool is actuated to re-sect the tissues. The nerve stimulating monopole filament can direct the course of tissue resection upon reaching boundary pixels of the tumour.

In summary, the sub-components of the Rotitome-G are assembled and embedded in the outer housing of the instrument. It includes optical fibres for the camera, LED, infrared inductance transducer, monopole filament, electromagnetic solenoids, and ultrasonic micro-transducer. The internal flexible torque shaft assembly carries cables for 360-degree retro-flexion, steering, sweeping and grazing motions of the steerable head. The external assembly in the static outer housing is within a shrink wrap sheath and the central assembly rotates concentrically relative to its internal surface. The flexible distal end of the outer housing that otherwise follows the movements of the cutting head may be locked in an optimal position once the angle of attack is set to allow the protruding cutting head to sweep and graze for effective resection of the tumour tissues.

4.0 Biomechanical properties of the brain tissue

The brain neural tissue is an intricate network of heterogeneous parenchyma made-up of neurons, nerve tracts, and active glial cells in its matrix. The highly vascular brain is suspended in cerebrospinal fluid (CSF) enclosed in three serous membranes, including Dura mater, Arachnoid, and Pia mater. The ventricular system of the brain filled with circulating CSF communicates with the spinal canal act like intrinsic cushion to provide strain relief, preventing tissue distortion (Ivarsson J, 2000). Within confines of the cranium, under normal physiological conditions, there is a fine volumetric balance to maintain normal intracranial pressure to protect incompressible tissues of the brain. The understanding of mechanical properties of the brain tissues is important to realize the effect of patient positioning with an intracranial tumour, craniotomy, breaching of Dura mater, and manipulation of the organ with instruments during surgery.

Although soft to touch but from an engineering perspective, the brain is a solid organ. The viscoelastic tissues of the brain behave in a highly non-linear fashion. The organ is strain-rate sensitive and time-dependent mechanical response is based on the rate and magnitude of applied load (Bilston et al., 2008). The properties of neural tissues change substantially due to surgical injury and tissue manipulation causing osmotic changes and cerebral oedema (Cheng et al., 2008). For practical neurosurgical purposes, the brain shows a linear very small sinusoidal response with compressive indentations as small as 25 microns and non-linear with compression equivalent to 300 microns. The compression of brain tissues accompanied by shear, show linear viscoelastic storage, loss of elasticity and get stiffer as the rate of loading increases (Fallenstein et al., 1969). However, as the shear strains exceed the linear viscoelastic limit, the brain shows shear thinning behaviour, becoming softer as relaxation modulus decrease with increasing strain (Takhounts et al., 2003). Under constant strain rate, the brain tissue can sustain larger strains without macroscopic changes in structure. The

onset of yield or failure occurs when the change caused by compression exceed 30-50% of the original volume of the tissues under strain(Atsutaka Tamura. et al., 2007).

The brain appears to soften with age in adults and tumours may be distinguished from the healthy structures based on rheological properties in the living with MRI elastography technique(Xu et al., 2007). The white matter is largely homogeneous and isotropic while other regions are anisotropic with a change in the direction of the tracts and the distinction between normal and abnormal may be due to differences in elastic modulus and texture of the tissues(Xu et al., 2007).

5.0 Brain shift

In the supine position, on an axial MRI view the maximum brain translation is in the anterior-posterior direction due to the dependent position of the organ(Ivan et al., 2014). The shift in deep structures enclosed within the brain cortex can be up to 4 mm and the cortex may deform 10 mm or more(Kelly et al., 1986).

Craniotomy induced brain shift due to gravity, direct atmospheric pressure upon opening the Dura mater, loss of cerebral-spinal fluid, venous bleeding, cavity formation of tumor-space, the collapse of tumour walls, viscoelastic recovery of the healthy neural tissues, cerebral oedema, and surgical retraction are all attended with warping of the brain tissue(Gerard et al., 2017; Ivan et al., 2014; Roberts et al., 1998). The brain surface may warp up to 20 mm depth and exceed 50 mm depending on the size of the tumour cavity after resection(Hartkens et al., 2003). This non-linear mechanical phenomenon leads to miscalculation of pre-operative navigation targets during surgery reducing the precision of semiautomatic and automatic instruments, and difficulty in registration and segmentation of post-operative residual volume assessment of the tumour(Gerard et al., 2017). Minimizing the craniotomy access is one of the ways to reduce the extent of the brain shift and worsening of the deformation during tumour resection.

During minimal burr-hole craniotomy even when there is no need for brain retraction, on opening the Dura mater the brain shift occurs with entry of air due to loss of CSF to equalize intracranial and atmospheric pressure(Elias et al., 2007). It may happen even from a little force applied to insert a guide pin to pass surgical instruments(Ivan et al., 2014). The second pass of an instrument doubles the brain shift rate, so does the second portal and bilateral access. The size of the craniotomy affects the magnitude of brain warping(Maurer et al., 1998). A large craniotomy and sinking of the cortical surface due to gravity can be considerable(Iversen et al., 2018).

6.0 Relation of preoperative and intraoperative imaging

The interest in image processing and simulation techniques for patient-specific surgical planning has been much greater in planning neurosurgical procedures than other surgical specialties. This desirability is because of greater accuracy in localizing intracranial tumours and navigation of the surgical steps at the beginning and during the procedure. Therefore, the pre-operative planning process and intra-operative imaging technology form a continuum from the time of diagnosis to positioning of the brain before and after craniotomy. It helps to redefine the varying anatomy due to mechanical changes in the brain tissues because of cerebral-spinal fluid loss and space relaxation within and outside the tumour cavity as tumour resection proceeds(Nakaji & Spetzler, 2004). Computer-assisted image-guided systems rely on data collected during preoperative planning for intra-operative orientation and image registration. Consequently, the tumour space orientation of mechanically misbegotten shape of the brain as a new development during surgery cannot be safely managed based on image spatial coordinates acquired preoperatively. As the intra-operative CT has obvious drawbacks of radiation exposure and poor soft tissue differentiation ability the value of MRI as the primary diagnostic modality is beginning to be recognized as the intra-operative modality as well to monitor mechanical changes occurring during surgery(Black et al., 1997), which can demonstrate intracranial structures more precisely. However, high-resolution 3Tesla or higher strength MRI machines are associated with the risk of image distortion artifacts that can cause localization errors during navigation(Novotny et al., 2005). Considering increasing role of image processing and analysis for patient-specific pre-operative planning and intra-operative update during neurosurgical procedures the role of the Rotitome-G can be exploited further because of its assistive devices and pixel-level operating ability.

7.0 Neuronavigation



The first described neuronavigation technique in 1908 was a cranial stereotactic procedure, where a frame was directly screwed onto the skull to target cranial lesion based on Cartesian coordinate system (Rahman et al., 2009). Modern neuronavigation, in conjunction with intra-operative CT and MRI, is a computer-based technology to guide and navigate instruments within confines of closed space in the skull for surgical procedures. The technology allows spatial positioning of the patient (physical space), targets surgical devices at the pre-defined segmented region of interest and directs their motion which corresponds to virtual image space visualized on VDU to carry out the procedure. The advanced imaging technologies, computer graphic modeling, the advent of the graphic processing unit (GPU), and acceleration of data processing have made the spatial merger of the images possible through mathematical algorithms.

The pre-operative images are used to locate the intracranial lesion to site the craniotomy and carry out resection of the tumour. The frame-based neuronavigation system for neurosurgery use externally applied stereotactic apparatus attached to the head of the patient, and the frameless system employs either bony markers or markers adherent to the skin for image registration to acquire 3D co-ordinates for correspondence between the physical tumour space and virtual image space. While the frame-based method offers greater accuracy otherwise both methods have limitations (Woodworth et al., 2005). Soon after the patient positioning and creation of craniotomy, the brain shift leads to inaccuracies and relatively disrupts native anatomy, and hence the correspondences between physical tumour space and image space co-ordinates during surgery (Mittal & Black, 2006; Yrjänä et al., 2007). Combining neuronavigation with intraoperative MRI enables to optimize surgical course to avoid vital functional structures in the immediate vicinity when extending the procedure to remove residual tumour tissue (Nimsky et al., 2001).

The specially developed open-access software such as 3D-Slicer (www.slicer.org) can be fully integrated into the navigation system combining pre- and intra-operative images for a continuum of the technique throughout the surgery. This helps to attain similarity in the coordinates of the physical tumour-space and virtual image-space when corresponding intra-operative magnetic resonance images are used for tumour update and adjustment of the surgical instruments interactively. Applying the same imaging modality before and during surgery may reduce the computational cost in the registration process of the warped images generated during surgery. Similarly, the segmentation process facilitates navigation and orientation of coordinates of the real intracranial tumour-space and virtual image-space on a VDU for greater understanding to reduce errors.

Segmentation and 3D computer modeling allow morphometric measurements and spatial framework during surgery. For the finite element analysis, following meshing of the image domain for finite element modeling relevant boundary conditions and loading conditions can be applied before and after the simulated craniotomy. It would help to assess the brain tissue deformation during surgery to plan the motion of interactive and automatic surgical instruments. Nonetheless, there will always be surprises to steer the course of the surgery despite patient-specific preoperative planning and careful computer modeling and mathematical algorithms to run the navigation set up to perform the surgery interactively or automatically.

With piecemeal removal of tumour, there will be gradual intrinsic recoil and collapse of the compressed effaced cerebral tissues into the tumour cavity. The brain shift is an unpredictable time-dependent phenomenon due to the time lag between patient positioning and incision of the Dura mater, size of craniotomy, first pass of an instrument and the increasing volume of the tumour cavity. The intraoperative navigation and structural MRI can help calculate precise brain shift and its deformation for correspondence of updated tumour space geometry and image space coordinates in relation to the remainder of the brain parenchyma (Iseki et al., 2008). Suggestively, the incorporation of a robotic neurosurgical technique would help achieve highly selective resection within 10 micro-meter precision and bring opportunities to manipulate tissues within limited intracranial space (Iseki et al., 2008). Simple steps such as neuronavigation set up in advance, minimal size craniotomy access, the image-guided optimal positioning of stylet and sheath, and watertight seal as described below can help prevent initial translation and deformation of the brain surface.

Magnetic resonance imaging is a preferred diagnostic modality preoperatively and intraoperatively to mitigate difficult scenarios and have a similarity of navigation control points or fiducials. The use of intraoperative ultrasound is less than optimum because hyper-echoic shadows from the tumour may be confused with a similar intensity gradient of the preoperative image at the borders between different anatomic structures (Iversen et al., 2018). The differentiation becomes even more difficult if tumour boundaries are diffuse and an intensity-based segmentation algorithm is used for image correspondences. For the safety and effectiveness of a surgical procedure patient-specific and patient-appropriate pre-operative planning is recommended.

An awakened patient craniotomy, neuronavigation, target access surgery with correspondences of intraoperative structural MRI and pre-operative functional MRI is a reasonable approach to resect brain tumours to avoid eloquent brain areas. An awakened patient craniotomy also allows somatic-sensory and direct motor stimulation at the cortical and sub-cortical levels.

8.0 Surgical principles for resection of glioma tumour and tumour enhancing modalities

The glioma tumours arise from supporting glial cells and glioblastoma is the most frequent and malignant tumour having extremely poor prognosis (Barnholtz-Sloan et al., 2018; Wen & Kesari, 2008). Reducing the bulk or maximum gross resection of these tumours provides the best possible progression-free period post-operatively and short-term survival depending on WHO grade I to IV (Y. M. Li et al., 2016). The length of survival is not only based on low and high-grade tumours but is closely associated with the extent of surgical resection (Sanai & Berger, 2008). The progression of the lesion and preservation of the neurological function after surgery is equally important for the quality of life during the remainder of the life span of the patient (McGirt et al., 2009). There are multiple modalities available to neurosurgeons to maximize the extent of tumour resection and leave behind minimal residual malignant tissue to protect salient functions and eloquent areas in the vicinity of the tumour (De Witt Hamer et al., 2012; Wu et al., 2007). The contrast-enhanced MRI defines anatomy and characteristics of high-grade glioma and T₂ weighted or fluid attenuation inverse on recovery (FLAIR) signal MRI enhances low-grade tumours of the glial tissue. The diffusion tensor imaging and functional MRI when done pre-operatively helps to identify descending motor tracts and specific active areas in the brain, particularly to preserve language function, by detecting higher blood flow to these areas (Ogawa et al., 1992). T₂-based MRI diffusion tensor imaging (tractography) measures the diffusion of water molecules along the axis of the axons and its direction varies with anisotropy and heterogeneity of the descending tracts from the cortex to the spinal cord (Basser et al., 1994). To maximize tumour resection preoperative localization of these tracts during pre-surgical planning can significantly help intraoperative registration to the structural MRI.

Frequently due to the infiltrative nature of the glioma tumour the distinction from the normal neural tissues can be very difficult. To increase visual differentiation fluorescence photodynamic methods are used. One of the prevalent fluorophores is 5 Amino-Levulenic Acid (5-ALA), which stains high-grade glioma for better visualization of tumour margins under ultraviolet light (Stummer et al., 1998). 5-ALA is a natural precursor of haemoglobin and accumulates preferentially as fluorescent protoporphyrin IX in active malignant cells (Regula et al., 1995). However, 5ALA cannot demark the boundary between malignant and eloquent tissue due to variability in uptake depending on the mitotic activity of tumour tissues (Jenkinson et al., 2018). In addition, adverse pharmacological effects of 5-ALA are nausea, mild hypertension, elevated liver enzymes, photosensitivity, and neurological deficits (Mansouri et al., 2016).

Therefore, Gadolinium-enhanced intraoperative MRI T₁ weighted images and T₂ weighted non-enhanced FLAIR images to discover satellite lesions to decrease the residual volume of the tumour is recommended. There may be a synergistic effect of the combined application of 5-ALA and intraoperative MRI (Tsugu et al., 2011). There are reports of 99.7% resections in eloquent brain areas by employing these new modalities (Reyns et al., 2017). The limitation to wider resection – supramarginal excision (Yan et al., 2017) of these invasive tumours is the immediate presence of vulnerable eloquent brain areas. The benefit of employing technologies such as intra-operative structural MRI and 5-ALA, in maximizing the extent of tumour resection in cases of high-grade glioma is uncertain because the available evidence is of low quality (Jenkinson et al., 2018).

It is the heterogeneity of the tumour tissue and satellite formation that unnerves even the most experienced neurosurgeon when faced with infiltrating tumours. No matter what the extent of tumour resection and available apparatus, the surgery for glioblastoma is incurable currently. The most important surgical principle is the experience of the operating surgeon.

9.0 Application of Rotitome-G to resect intracranial tumours

The Rotitome-G is based on biomimetic ideology for pixelwise resection in the tumour space of an intracranial tumour with its micro-endoscope, micro-cutting tool variations, and assistive devices erasing of one or more pixels at a time in the image space to achieve complete resection of a tumour. The cutting head advances in the tumour space corresponding to the image space cursor movements desired by the operator equivalent to the area of a pixel (0.26×0.26mm) represented in the image. The depth of the cutting tool is equal to the

thickness of the image slice, generally 0.625mm in the case of computed tomography. Ideally, it would be preferable if the slice thickness is matched to the depth of a pixel-sized cube (voxel) for greater precision, resulting in the erasure of a complete voxel thick layer in the physical space. This will avoid discrepancy between the erasure of a voxel-sized depth in the image space of a displayed slice and incomplete excision of the real-world tissue layer when the next slice is displayed in the image space. Alternatively, the cutting depth of the tool is adjusted to match the exact thickness of the CT slice and as each pixel is erased in the image space the thickness of the tissue layer excised in the physical space is equal to the thickness of the image slice. As this would reduce the precision, therefore there is a need for CT scanners to produce each slice as thick as the depth of a pixel or the pixel size is changed to $0.625 \times 0.625\text{mm}$, which would reduce the image resolution even at 100% magnification. The sub-cellular level micro vision of the tumour tissue in the physical space is enhanced by assistive devices to precisely locate and segregate tumour tissue from the normal and more importantly eloquent areas of the brain.

The movements of the cutting tool follow the actuation of the instrument head controlled manually or by a robotic arm programmed during pre-operative simulation of pixel-by-pixel tumour resection, and the data collected is transferred to navigation set up during surgery. The dataset can be updated as required during registration of pre-operative and intraoperative structural, functional, and diffusion tensor MRIs to match with the change in orientation due to deformation of tumour anatomy and evolution of brain shift as resected space gets larger. The head of the instrument has universal articulation with the rotating shaft constructed by stacking multiple layers of titanium spheres to produce differential motion to allow smooth deflection of the steerable head. The articulation can be locked in multiple positions to effect controlled tissue excision. The required length of the micro-endoscope head is presented within the tumour cavity as it gets larger to reach the remainder of the tumour (Fig. 4). The depth of incursion is achieved by a precise feedback mechanism provided by the non-tactile infrared inductance sensor and monopole nerve stimulating monofilament.

To increase the precision of the resection process it is important to have the provision of intraoperative MRI to correspondingly update both the tumour space and image space. As the resection of the tumour proceeds, if there is brain shift then steerable and sweeping action of the cutting head of the instrument in the tumour space would require a frequent update for image registration and segmentation. It is to realign the coordinates of the image space to the tumour space so that the erasure of pixels (pixelectomy) correspond to the tumour tissue for resection. For effective cutting of the tissue the face of the cutting tool should be normal to the tissue plane and updated regularly on each 2D slice in the MRI image space. Once in the desired position the instrument may be set to automatic mode under visual supervision in the central zones and performed manually at the periphery of the tumour with sub-cellular level micro-endoscopic examination and as directed by nerve stimulation probe and infrared inductance. The tumour resection can be completed successfully with the collaboration of the surgeon monitoring the tumour space and the clinical biomechanical engineer handling the image space update for correspondence in consultation with a radiologist.

The motion of the cutting tool is designed to remove the tumour tissue by sweeping and grazing over the entire tissue plane of each image slice from top to bottom and from left to right of the tumour mass in correspondence with MRI slices. For each 2D image slice, the cutting tool follows the magnified image plane in the form of a raster image grid pattern according to X and Y coordinates. After the excision of each plane, the cutting head descends to the next plane in the Z direction, as programmed during pre-operative construction of a 3D virtual model of the tumour. This pixelectomy level tumour excision can be viewed as inverse of the layer-by-layer additive manufacturing process based on standard tessellation language file prepared preoperatively to semi-automatically excise 2D stereoscopic tumour pixels or 3D voxels. Such an in-silico activity can bring a dual advantage, first providing 3D reconstruction for excision of pathological tissue of a selected anatomical site, and secondly, the same standard tessellation language file dataset can act as stereo tessellation lithography (STL) file preoperatively to create a tumour model with additive manufacturing.

The robotic mechanism can be applied for the movements of the head and neck of the fibre-optic Rotitome-G housed in the rigid cannula fixed at the craniotomy portal to facilitate its actuation. The rate of tissue resection is semiautomatic and updated during surgery as desired by the operator with changing geometry of the tumour space. The steerable head works continuously following the shortest distance on the cut surface of the tumour to graze and sweep within the tumour space according to pre-operative plan or as updated intra-operatively. If the resection proceeds according to the plan, then resection of the tumour continues pixel-by-pixel (voxel-by-voxel) in the in the tumour space corresponding to pixelwise erasure in the image space sharing the same geometrical coordinates. However, in the case of rhizoid infiltration of the tumour operator supervision is necessary.

The central aspirating channel is automatically activated with the actuation of the rotary cutting tool to aspirate the cut tissue bolus at an optimum vacuum pressure to prevent rupture of the tissues and haemorrhage. The aspirating canal can be connected to hyper-osmotic/hypertonic fluid source via a two-way operator-controlled stop-cock for lavage and aspiration accessible within the sterile field. The fluid must be delivered under gravity to prevent absorption adding to the pre-existing cerebral oedema that may worsen otherwise due to surgical injury and manipulation of the brain tissue. Intra-operative adverse effects of brain shift contributed by the collapse of the progressively enlarging cavity of the tumour may be mitigated by delivering cerebral spinal fluid analogue (a patentable intellectual property) or one of the experimental hyper-osmotic fatty acids at the end of the procedure. The cavity filling fluid must be clear to maintain the visibility of the tissue, preferably replaced continuously to remove the debris. At the completion of the resection, the tumour cavity may be left filled with a hyperosmotic/hypertonic solution or CSF analogue and drained gradually over the next 24 hours. It may be left longer depending on the size of the intracranial negative space to prevent haemorrhage and haematoma formation in the vacant space.

The micro-photonics infrared inductance transducer to measure the density of the tumour material can set the rotary speed appropriately based on tissue density feedback to effectively remove softened necrosed tissue and schirrous abnormal tumour tissue. The design of the Rotitome-G in the image space performs pixelectomy at a maximum of 6400 times magnification raster image to facilitate resection of the tumour tissue at the cellular level in the tumour space. In case the coordinates of the image and tumour plane are the same over a large area of the tumour and the expected trajectory to re-sect the tumour remains the same then the cutting tool may be locked in position for resection of the tumour in its reach. To avoid miscalculation at the edge pixels of the segmented region sensory transducer, cutting tool speed, and nerve stimulation feedback information help to increase the safety of the Rotitome-G during resection close to eloquent tissues. Although the feedback mechanism would either redirect the tool or halt the resection process, but the motion of the cutting face must be monitored very closely. In addition to the existing assistive devices, it is possible to include a temperature sensor to distinguish tumour tissue from healthy areas of the brain. To these assistive devices, an alarm may be added to warn the operator in case the cutting tool is too close to eloquent areas and allow manual intervention by the operator.

10.0 Rotitome-G instrument placement and practice of the HSG-Amoeba technique

Traditionally, the scalp incision and craniotomy flap are 2 to 4cm larger than the measured size of the tumour for placement of the cortical mapping mat. When it comes to resecting invasive tumour tissue and significant pre-existing neurological deficit direct piecemeal resection technique is preferred. However, endoscopic technique is favored in limited anatomical zones and bilateral butterfly intracranial tumours saddled across the mid-sagittal plane(Hoshide & Teo, 2017). In this regard, target access intracranial micro-endoscopy for resection of glial tumours would be a clear advancement when it comes to resect ambiguous invasive tumour tissue. The time-dependent mechanical global shift in the brain and sub-cortical tissues is another significant occurrence in cases of sizable tumours during the progression of the tumour surgery. This issue has been largely overcome with the introduction of intra-operative imaging(Senft et al., 2011) and frequent updates through the neuronavigation process. 5-ALA fluorescence of the tumour tissue also facilitates visualization independent of stereotactic neuronavigation guidance(Panciani et al., 2012).

Generally, distinguishing invasive denser and stiffer malignant tissue from the normal healthy tissues with unaided eyes is a surgical problem. The problem of physical characteristics of a tumour may be learned at the time of preoperative planning and segmentation process by employing techniques such as the hyalite sol-gel Amoeba (HSG-Amoeba) technique(Gandhi, 2022b) to determine tissue heterogeneity and to create a tissue density map and calculate elastic modulus by applying a soft tissue power law equation preoperatively. Application of the HSG-Amoeba technique for image segmentation of 2D CT slices based on image intensity has the advantage of providing distribution of tissue densities obtained during its apoptosis stage to distinguish tumour from normal neural tissues during surgical excision. The collected density and elastic modulus dataset can then be used intra-operatively for the application of a tactile or non-tactile sensing device to measure force for correspondence to tissue densities. Thus, the tactile information may assist by assessing relative stress distribution between residual tumour and normal brain tissues from prior knowledge of tumor tissue density.

Performing the surgery under awakened craniotomy or general anaesthesia is a surgical decision at the pre-planning stage. Frameless neuronavigation stereotactic setup allows to employ preoperative imaging, functional MRI, and diffusion tensor imaging. At the time of portal creation and entry it helps to direct initial

targeting of obturator and cannula assembly in relation to the eloquent cortical and subcortical anatomy. The frameless stereotactic system helps to establish the correspondence of coordinates between the preoperative images and the current surgical orientation of the target site of the organ (Blond et al., 1991). It is preferable to perform minimally invasive endoscopic surgery for tumour resection procedures within the MRI gantry space under a sterile environment rather than mobilizing the patient for intraoperative MRI imaging.

The head of the patient is secured rigidly in a non-metallic carbon fibre head fixation frame designed either for coupling to the MRI gantry or the operating table, such that it allows the patient in a supine, prone or decubitus position with preferred extension or flexion of the head based on the topography and anatomy of the tumour. Whatever the chosen position of the patient, the site of the lesion should be isocentric with the MRI gantry so that the spatial geometric coordinates of the physical tumour space are easy to match with the image space when the preoperative and intraoperative images require registration initially and during the procedure. The surgical site may be oriented globally either in conjunction with imaging modality mounted spherical magnetic compass or still better aligned to global positioning system (GPS) if the procedure is being performed at a remote location under MRI. The navigation within 3D physical space can be managed by having an image space console like an airplane flying instrument panel to control the cutting head movements of the Rotitome-G relative to the image plane.

Once the position of the patient and the head is rigidly stabilized in a frame the coordinates of the anatomical control points on the head are registered to virtual image anatomy in the image space. The locating probe is used to establish the salient anatomy landmarks to navigate with infra-red or radio frequency detection system (H. Taniguchi et al., 2006). The Rotitome-G has electromagnetic solenoids built into the instrument for tumour-space navigation. The Rotitome-G instrument is designed to automatically co-register with the intraoperative neuronavigation system and follows intraoperative updates as well as an unpredictable shift in the descending cortical-spinal tracts and other areas of concern during surgery.

After the skin preparation transparent radio-opaque grid (²TROG-G) adhesive film with embedded radio-opaque markers is applied to the shaved scalp. A 15mm craniotomy is made and the specially designed titanium watertight cranial portal device (³CPD) (Fig. 5) is screwed into the craniotomy hole to engage both the tables of the skull bone. The Dura mater may be incised in advance before inserting the screw-on CPD to deal with any likely surface blood vessels in the trajectory of the operating cannula. The CPD has an outer ring socket and an inner removable plug. The outer pocket has a watertight flexible diaphragm next to the Dura mater, which can be incised at the time of the entry of the non-ferrous trocar-cannula assembly of suitable length. The operating cannula is locked to the socket ring in place of the plug to steady it in position after making a suitable incision in the diaphragm after the track is created in a safe trajectory with navigable blunt trocars of graded diameters gradually enlarging the passage to access the subcortical tumour (Fig. 4). Once the target access surgical path is established the Rotitome-G flexible micro-endoscope is lowered into the cannula to the tumour space corresponding to the image space. The image is magnified up to 6400 times and the cutting tool is set to focus on the pixels corresponding to the focal tumour space before actuating the cutting tool.

Based on neuronavigation principles the relationship between the coordinates is maintained throughout and imaging is performed to correctly identify region-of-interest. The image segmentation is refreshed for the brain shift, and the tumour space is once again corresponded to the image space. Superficial and deep salient structures in the vicinity of the tumour are segmented and labeled as regions external to the region of interest to better define the 3D tumour specific space.

The concept of the HSG-Amoeba model is to include image segmentation, construction of 3D tumour model for finite element analysis, and extracting distribution of the tissue densities to formulate material properties. The micro-endoscopic instrument Rotitome-G with its unique cutting variations and assistive devices is designed to safely permit complete pixel-level resection of the tumour in the physical space.

11.0 Discussion

Surgery is going to remain the most important step in the management of malignant tumours in conjunction with radiotherapy and chemotherapy treatments. The main objective of surgery is maximum resection of

² Intellectual property of the author

³ Intellectual property of the author



invading tumour tissue for cytoreduction, to reduce the chances of disease progression, improve quality of life and overall prognosis. For such attainments what concerns an operating surgeon most is to achieve maximum malignant tissue excision with minimum damage to the normal tissues and eloquent areas in the case of a brain tumour. The only way ahead to get a visible clearance of invading rhizoid spread of tumour tissue is to employ all technologies currently available for safe application to shift the present surgical ideals in treating not only the intracranial tumours but all other tumours situated deep in the body cavities.

Oncology surgery is based on best possible characterization of abnormal tissues by special means to recognize them with or without aid to enhance macroscopic as well microscopic appearance to increase the potential of an operating surgeon. Grossly, the physical characteristics of almost all the tumours are certainly different from the normal tissues in the neighbourhood. However, the human eye cannot see beyond the surface characteristics and certainly does not have microscopic and x-ray vision and has no sensory means to recognize density and chemical nature to excise infiltrating tissues unaided. The human eye has a visual spectrum range of 400-750 nanometers with a resolution of 50 micrometers, and a limited spectrum to recognize closely related shades of colour and grey tones of the tissues with naked eyes (Harlaar et al., 2014). The same applies when it comes to palpating the elastic nature or stiffness of residual tissues directly to distinguish normal from the abnormal visually without prior knowledge. Therefore, to improve the ability to recognize and protect the normal tissues several technologies such as tissue fluorescence, pre-operative and intraoperative imaging, computer vision, and navigation system; and microsurgical techniques have been developed to increase the extent of resection of a tumour. The combined application of these sophisticated technologies is the only means to develop further strategies to target pathological anatomy, and at the same time detect residual tumour volume and avoid blood vessels, nerves, and eloquent areas.

The most unnerving consequence of the traditional wide operative field approach despite the advanced intra-operative imaging modalities is the failure to recognize and distinguish invisible abnormal infiltrating tissues at the periphery for safe resection. One remedy to mitigate the issue of visibility is the magnification of the surgical anatomy with an operating microscope to enhance visual differentiation between the normal and tumour margins to extend the resection (Yasargil & MG, 1969). The next step to narrow the surgical corridor is accessing body compartments with rigid endoscopic equipment with two or more portals demanding significant surgeon skills and coordination for precision and accuracy. The flexible endoscopes are now fitted with high-definition CCD cameras, visual display units to visualize images in real-time, which can be easily fitted with tracking sensors and maneuvered under direct virtual vision during surgery.

The flexible Rotitome-G micro-endoscope can directly access the interior of an organ within closed body cavities under the integrated intra-operative image guidance. It is directed by a navigation system from the beginning to the end for a satisfactory extent of tumour resection. The Rotitome-G micro-endoscope makes the direct microscopic subcellular view of the tumour tissues possible, and the resection is carried out at pixel (voxel) level by aligning patient tumour coordinates to the image space co-ordinate in 2D areal image segmentation and co-registration update on residual tumour and organ anatomy during surgery. The Rotitome-G comes with assistive devices for characterization of the tissues to separate abnormal from the normal eloquent areas when approaching most peripheral margins of the tumour, not only through direct microscopic visualization but also direct nerve stimulation and tissue impedance before application of the cutting tool. Integration of imaging modalities and navigation system to monitor the motion of the Rotitome-G head with its cutting tool increases the ability to perform excision of tumour pixel-by-pixel by adapting to the registered 2D cross-section slices to the 3D rendering of the pathological anatomy.

The Rotitome-G concept is designed to be compatible with the surgical robotic mechanism. This provision is included to increase the precision between the operator interface at the pixel-level image space and its motion based on electromagnetic solenoid sensors at the leading end within the tumour-space or similar pathological anatomical space. There is no surgical robot that can substitute the surgical skills of a well-trained surgeon, whose dexterity comes with more than 24 degrees of freedom occurring at small and large articulations controlled by numerous muscles producing coordinated motions of upper extremities (Motkoski & Sutherland, 2014). A robot must be programmed to prevent inadvertent injury to the eloquent tissues within and outside the operative tumour volume. For a successful outcome of the Rotitome-G based surgical resection, a patient-specific 3D model needs to be built from pre-operative imaging data with appropriate segmentation and registration for tracking it, so that it can be visualized within the virtual model. The physical coordinates of the patient are fixed in one position to perform endoscopic surgery to assist steerable sweeping action in multiple directions to graze and excise the tissue as more and more pixels are erased in the image space. The infrared impedance transducer device in the head of the Rotitome-G helps recognize tissue density. The robotic arm has limitations to register and provide true haptic feedback from the actual surgical site surface to mimic force

recognition like touch and pressure senses of a surgeon. Where robotic arm-based surgery is planned, application of the HSC-Amoeba technique can segment the region of interest, provide tissue density and material properties for haptic feedback to the sensory system of the operating robot from the calculated density and impedance values.

Currently, for microsurgical resection of intracranial tumours in large centres diffusion tensor MRI and fMRI are employed in conjunction with navigation to optimize the surgical outcome. The primary purpose of image processing is co-registration of image and patient-based pathological anatomy coordinates. It helps to develop a common reference frame for visualization and navigation of surgical instruments and patient movements during awakened surgery. However, registration of images in the form of 2D slices of changing anatomy during the progression of surgery often comes with occlusion of irregular infiltrating tumour tissues and displacement of eloquent areas due to brain shift. All areas may not be visualized in all cross-sectional 2D slices. It demands careful recognition of pixel inclusion by refreshing segmentation for pixel erasure and precise excision of tumour tissue. The issue of occlusion of important anatomy raises challenges when pixel-level erasure and tissue excision are performed within the same geometrical co-ordinates at the periphery of the pathology. There will be blind spots at the ceiling of the tumour space near the area where the endoscope makes its entry and begins excision of the tumour tissue, despite its retro-flexion capability. Most if not all the tissues may still be excised by using the cutting tool of the Rotitome-G manually. It calls for surgeon-based experience and understanding of infiltrating tumour tissue from pre-operative images and the ability to relate to the updated intra-operative imaging modality in use. Therefore, pre-operative planning should preferably include rigorous patient-specific computational biomechanical implications from the finite element analysis (Wittek et al., 2016) and simulation of the surgery. It is an interdisciplinary effort in collaboration with an experienced clinical biomechanical engineer and a team consisting of radiologist and neurologist/neurosurgeon to understand the deformation of white matter tracts on diffusion tensor MRI and f-MRI (Schonberg et al., 2006). Then only target access surgery with the Rotitome-G micro-endoscope can be successful.

12. Conclusion

Seventy percent of the gliomas according to WHO classification belong to grades 3 and 4 (Kleihues et al., 2002). The goal of neurosurgical resection is to excise the maximum amount of pathological tissue, and minimal damage to the eloquent areas at the microscopic level to improve prognosis and limit neurological morbidity. Therefore, the key design of the Rotitome-G and the built-in assistive devices reflects to meet these surgical goals when combined with pre-operative surgical planning and computational biomechanics of the brain. For correspondence of preoperative and intraoperative images, there is a need for a suitable intra-operative imaging modality and software to undertake image segmentation and registration, to clearly define 2D cross-sectional anatomy of local pathology and global organ anatomy during surgery.

Originality: To the knowledge of the author the bringing together of various functional components to construct the concept of Rotitome-G, the micro-endoscope, and other accessories described are original and their arrangement is intellectual property of the author. All the figures are original except for the modified section of the cerebral cortex with placement of the Rotitome-G in the fig. 4. Its legend carries the reference details of its source.

Conflict of interest: The author declares that there is no conflict of interest.

References

- Atsutaka Tamura., Hayashi, S., Nagayama, K., & Watanabe, I. (2007). Mechanical Characterization of Brain Tissue in High-Rate Compression. *J Biomech. Sci Eng*, 2(3), 115–126. <https://doi.org/DOI:10.1299/jbse.2.115>
- Ainger, R., & Gillquist, J. (n.d.). *Arthroscopy of the knee*. Thieme Medical Publishers, 1991, New York.
- Barnholtz-Sloan, J. S., Ostrom, Q. T., & Cote, D. (2018). Epidemiology of Brain Tumors. In *Neurologic Clinics*. <https://doi.org/10.1016/j.ncl.2018.04.001>



- Basser, P. J., Mattiello, J., & LeBihan, D. (1994). MR diffusion tensor spectroscopy and imaging. *Biophysical Journal*. [https://doi.org/10.1016/S0006-3495\(94\)80775-1](https://doi.org/10.1016/S0006-3495(94)80775-1)
- Bedard, N., Quang, T., Schmeler, K., Richards-Kortum, R., & Tkaczyk, T. S. (2012). Real-time video mosaicing with a high-resolution microendoscope. *Biomedical Optics Express*. <https://doi.org/10.1364/boe.3.002428>
- Bhandari, A., Koppen, J., & Agzarian, M. (2020). Convolutional neural networks for brain tumour segmentation. *Insights into Imaging*, 11(1). <https://doi.org/10.1186/s13244-020-00869-4>
- Bilston, L., Clarke, E., & Cheng, S. (2008). Brain tissue mechanical properties – making sense of 5 decades of test data. In A. Gefen (Ed.), *The pathomechanics of tissue injury and disease, and the mechano-physiology of healing* (pp. 1–18). Kerala Research Sign Post.
- Black, P. M. L., Moriarty, T., Alexander, E., Stieg, P., Woodard, E. J., Gleason, P. L., Martin, C. H., Kikinis, R., Schwartz, R. B., & Jolesz, F. A. (1997). Development and implementation of intraoperative magnetic resonance imaging and its neurosurgical applications. *Neurosurgery*. <https://doi.org/10.1097/00006123-199710000-00013>
- Blond, S., Lejeune, J. P., Dupard, T., Parent, M., Clarisse, J., & Christiaens, J. L. (1991). The stereotactic approach to brain stem lesions: a follow-up of 29 cases. *Acta Neurochirurgica. Supplementum*. https://doi.org/10.1007/978-3-7091-9160-6_21
- Carton, F.-X., Chabanas, M., le Lann, F., & Noble, J. H. (2020). Automatic segmentation of brain tumor resections in intraoperative ultrasound images using U-Net. *Journal of Medical Imaging*, 7(03). <https://doi.org/10.1117/1.jmi.7.3.031503>
- Cheng, S., Clarke, E. C., & Bilston, L. E. (2008). Rheological properties of the tissues of the central nervous system: A review. In *Medical Engineering and Physics*. <https://doi.org/10.1016/j.medengphy.2008.06.003>
- Coté, G. L., Lec, R. M., & Pishko, M. V. (2003). Emerging biomedical sensing technologies and their applications. *IEEE Sensors Journal*. <https://doi.org/10.1109/JSEN.2003.814656>
- De Witt Hamer, P. C., Robles, S. G., Zwinderman, A. H., Duffau, H., & Berger, M. S. (2012). Impact of intraoperative stimulation brain mapping on glioma surgery outcome: A meta-analysis. In *Journal of Clinical Oncology*. <https://doi.org/10.1200/JCO.2011.38.4818>
- Elias, W. J., Fu, K. M., & Frysinger, R. C. (2007). Cortical and subcortical brain shift during stereotactic procedures. *Journal of Neurosurgery*. <https://doi.org/10.3171/JNS-07/11/0983>
- Fallenstein, G. T., Hulce, V. D., & Melvin, J. W. (1969). Dynamic mechanical properties of human brain tissue. *Journal of Biomechanics*. [https://doi.org/10.1016/0021-9290\(69\)90079-7](https://doi.org/10.1016/0021-9290(69)90079-7)
- Gandhi, H. S. (2022a). A Comprehensive Review of Computer Vision Techniques to Interest Physicians and Surgeons, Role of A Clinical Biomechanical Engineer in Pre-Operative Surgical Planning, And Preamble To HSG-Amoeba, A New Concept of Biomedical Image Modeling Technique. *International Journal of Computers and Technology*, Vol. 22 (2022), 1–49. <https://doi.org/10.24297/ijct.v22i.9219>
- Gandhi, H. S. (2022b). Hyalite Sol-Gel Amoeba: A Physiology-Based Biophysical Model for Segmentation and Biotransformation of Medical Images To 3D Solid-State Characterizing Native Tissue Properties for Patient-Specific and Patient-Appropriate Analysis for Surgical Applications. *International Journal of Computers & Technology*, 22, 64–85. <https://doi.org/10.24297/ijct.v22i.9228>

- Gerard, I. J., Kersten-Oertel, M., Petrecca, K., Sirhan, D., Hall, J. A., & Collins, D. L. (2017). Brain shift in neuronavigation of brain tumors: A review. In *Medical Image Analysis*. <https://doi.org/10.1016/j.media.2016.08.007>
- Gergel, I., Hering, J., Tetzlaff, R., Meinzer, H. P., & Wegner, I. (2011). An electromagnetic navigation system for transbronchial interventions with a novel approach to respiratory motion compensation. *Medical Physics*. <https://doi.org/10.1118/1.3662871>
- Grant, B. D., Quang, T., Possati-Resende, J. C., Scapulatempo-Neto, C., de Macedo Matsushita, G., Mauad, E. C., Stoler, M. H., Castle, P. E., Guerreiro Fregnani, J. H. T., Schmeler, K. M., & Richards-Kortum, R. (2019). A mobile-phone based high-resolution microendoscope to image cervical precancer. *PLoS ONE*. <https://doi.org/10.1371/journal.pone.0211045>
- Harlaar, N., van Dam, G., & Ntziachristos, V. (2014). Intraoperative optical imaging. In F. A. Jolesz (Ed.), *Intraoperative Imaging and Image-Guided Therapy* (pp. 233–245). Springer Science+Business Media.
- Hartkens, T., Hill, D. L. G., Castellano-Smith, A. D., Hawkes, D. J., Maurer, C. R., Martin, A. J., Hall, W. A., Liu, H., & Truwit, C. L. (2003). Measurement and analysis of brain deformation during neurosurgery. *IEEE Transactions on Medical Imaging*. <https://doi.org/10.1109/TMI.2002.806596>
- Hata, N. (2014). Surgical Navigation Technology. In F. Jolesz (Ed.), *Intraoperative Imaging and Image-Guided Therapy* (Ed, pp. 249–257). Springer Science+Business Media. https://doi.org/10.1007/978-1-4614-7657-3_17
- Hoshide, R., & Teo, C. (2017). Neuroendoscopy to Achieve Superior Glioma Resection Outcomes. *Clinical Neurosurgery*. <https://doi.org/10.1093/neuros/nyx274>
- Intraoperative Imaging and Image-Guided Therapy*. (2014). In *Intraoperative Imaging and Image-Guided Therapy*. <https://doi.org/10.1007/978-1-4614-7657-3>
- Iseki, H., Nakamura, R., Muragaki, Y., Suzuki, T., Chernov, M., Hori, T., & Takakura, K. (2008). Advanced computer-aided intraoperative technologies for information-guided surgical management of gliomas: Tokyo Women's Medical University Experience. *Minimally Invasive Neurosurgery*. <https://doi.org/10.1055/s-0028-1082333>
- Ivan, M. E., Yarlagadda, J., Saxena, A. P., Martin, A. J., Starr, P. A., Sootsman, W. K., & Larson, P. S. (2014). Brain shift during bur hole-based procedures using interventional MRI: Clinical article. *Journal of Neurosurgery*. <https://doi.org/10.3171/2014.3.JNS121312>
- Ivarsson J, V. D. C. L. P. (2000). Strain relief from the cerebral ventricles during head impact: Experimental studies on natural protection of the brain. *Journal of Biomechanics*, 33(2), 181–189.
- Iversen, D. H., Wein, W., Lindseth, F., Unsgård, G., & Reinertsen, I. (2018). Automatic Intraoperative Correction of Brain Shift for Accurate Neuronavigation. *World Neurosurgery*. <https://doi.org/10.1016/j.wneu.2018.09.012>
- Jenkinson, M. D., Barone, D. G., Bryant, A., Vale, L., Bulbeck, H., Lawrie, T. A., Hart, M. G., & Watts, C. (2018). Intraoperative imaging technology to maximise extent of resection for glioma. In *Cochrane Database of Systematic Reviews*. <https://doi.org/10.1002/14651858.CD012788.pub2>
- Jolesz, F. A., Lorensen, W. E., Shinmoto, H., Atsumi, H., Nakajima, S., Kavanaugh, P., Saiviroonporn, P., Seltzer, S. E., Silverman, S. G., Phillips, M., & Kikinis, R. (1997). Perspective. Interactive virtual endoscopy. In *American Journal of Roentgenology*. <https://doi.org/10.2214/ajr.169.5.9353433>

- Kacher, D. F., Whalen, B., Handa, A., & Jolesz, F. A. (2014). The Advanced Multimodality Image-Guided Operating (AMIGO) Suite. In *Intraoperative Imaging and Image-Guided Therapy*. https://doi.org/10.1007/978-1-4614-7657-3_24
- Karkenny, A. J., Mendelis, J. R., Geller, D. S., & Gomez, J. A. (2019). The Role of Intraoperative Navigation in Orthopaedic Surgery. *Journal of the American Academy of Orthopaedic Surgeons*. <https://doi.org/10.5435/jaaos-d-18-00478>
- Kelly, P. J., Kall, B. A., Goerss, S., & Earnest, F. (1986). Computer-assisted stereotaxic laser resection of intra-axial brain neoplasms. *Journal of Neurosurgery*. <https://doi.org/10.3171/jns.1986.64.3.0427>
- Khuri-Yakub, B. T., & Oralkan, Ö. (2011). Capacitive micromachined ultrasonic transducers for medical imaging and therapy. *Journal of Micromechanics and Microengineering*. <https://doi.org/10.1088/0960-1317/21/5/054004>
- Kleihues, P., Louis, D. N., Scheithauer, B. W., Rorke, L. B., Reifenberger, G., Burger, P. C., & Cavenee, W. K. (2002). The WHO classification of tumors of the nervous system. *Journal of Neuropathology and Experimental Neurology*. <https://doi.org/10.1093/jnen/61.3.215>
- Li, K. W., Nelson, C., Suk, I., & Jallo, G. I. (2005). Neuroendoscopy: past, present, and future. In *Neurosurgical focus* (Vol. 19, Issue 6). <https://doi.org/10.3171/foc.2005.19.6.2>
- Li, Y. M., Suki, D., Hess, K., & Sawaya, R. (2016). The influence of maximum safe resection of glioblastoma on survival in 1229 patients: Can we do better than gross-total resection? *Journal of Neurosurgery*. <https://doi.org/10.3171/2015.5.JNS142087>
- Mansouri, A., Mansouri, S., Hachem, L. D., Klironomos, G., Vogelbaum, M. A., Bernstein, M., & Zadeh, G. (2016). The role of 5-aminolevulinic acid in enhancing surgery for high-grade glioma, its current boundaries, and future perspectives: A systematic review. In *Cancer*. <https://doi.org/10.1002/cncr.30088>
- Maurer, C. R., Hill, D. L. G., Maciunas, R. J., Barwise, J. A., Fitzpatrick, J. M., & Wang, M. Y. (1998). Measurement of intraoperative brain surface deformation under a craniotomy. *Lecture Notes in Computer Science (Including Subseries Lecture Notes in Artificial Intelligence and Lecture Notes in Bioinformatics)*. <https://doi.org/10.1097/00006123-199809000-00066>
- McCirt, M. J., Mukherjee, D., Chaichana, K. L., Than, K. D., Weingart, J. D., & Quinones-Hinojosa, A. (2009). Association of surgically acquired motor and language deficits on overall survival after resection of glioblastoma multiforme. *Neurosurgery*. <https://doi.org/10.1227/01.NEU.0000349763.42238.E9>
- Mittal, S., & Black, P. M. (2006). Intraoperative magnetic resonance imaging in neurosurgery: the Brigham concept. In *Acta neurochirurgica. Supplement*. https://doi.org/10.1007/978-3-211-33303-7_11
- Motkoski, J., & Sutherland, G. (2014). Progress in Neurosurgical Robotics. In F. A. Jolesz (Ed.), *Intraoperative Imaging and Image-Guided Therapy* (ed, pp. 601–612). Springer Science+Business Media.
- Muldoon, T. J., Pierce, M. C., Nida, D. L., Williams, M. D., Gillenwater, A., & Richards-Kortum, R. (2007). Subcellular-resolution molecular imaging within living tissue by fiber microendoscopy. *Optics Express*. <https://doi.org/10.1364/oe.15.016413>
- Nakaji, P., & Spetzler, R. F. (2004). Innovations in surgical approach: the marriage of technique, technology, and judgment. *Clinical Neurosurgery*.

- Nimsky, C., Ganslandt, O., Kober, H., Buchfelder, M., & Fahlbusch, R. (2001). Intraoperative magnetic resonance imaging combined with neuronavigation: A new concept. *Neurosurgery*. <https://doi.org/10.1227/00006123-200105000-00023>
- Novotny, J., Vymazal, J., Novotny, J., Tlachacova, D., Schmitt, M., Chuda, P., Urgosik, D., & Liscak, R. (2005). Does new magnetic resonance imaging technology provide better geometrical accuracy during stereotactic imaging? *Journal of Neurosurgery*. https://doi.org/10.3171/jns.2005.102.s_supplement.0008
- Ogawa, S., Tank, D. W., Menon, R., Ellermann, J. M., Kim, S. G., Merkle, H., & Ugurbil, K. (1992). Intrinsic signal changes accompanying sensory stimulation: Functional brain mapping with magnetic resonance imaging. *Proceedings of the National Academy of Sciences of the United States of America*. <https://doi.org/10.1073/pnas.89.13.5951>
- Pallud, J., Varlet, P., Devaux, B., Geha, S., Badoual, M., Deroulers, C., Page, P., Dezamis, E., Dumas-Duport, C., & Roux, F. X. (2010). Diffuse low-grade oligodendrogliomas extend beyond MRI-defined abnormalities. *Neurology*. <https://doi.org/10.1212/WNL.Ob013e3181e04264>
- Panciani, P. P., Fontanella, M., Schatlo, B., Garbossa, D., Agnoletti, A., Ducati, A., & Lanotte, M. (2012). Fluorescence and image guided resection in high grade glioma. *Clinical Neurology and Neurosurgery*. <https://doi.org/10.1016/j.clineuro.2011.09.001>
- Pohl, K., Bouix, S., Shenton, M., Grimson, W., & Kikinis, R. (2007). Automatic segmentation using non-rigid registration. *Med Image Comput Comput Assist Interv*, 26(9), 1201–1212.
- Rahman, M., Murad, G. J. A., & Mocco, J. (2009). Early history of the stereotactic apparatus in neurosurgery. *Neurosurgical Focus*. <https://doi.org/10.3171/2009.7.FOCUS09118>
- Regula, J., MacRobert, A. J., Gorchein, A., Buonaccorsi, G. A., Thorpe, S. M., Spencer, G. M., Hatfield, A. R. W., & Bown, S. G. (1995). Photosensitisation and photodynamic therapy of oesophageal, duodenal, and colorectal tumours using 5 aminolaevulinic acid induced protoporphyrin IX - a pilot study. *Gut*. <https://doi.org/10.1136/gut.36.1.67>
- Reyns, N., Leroy, H. A., Delmaire, C., Derre, B., Le-Rhun, E., & Lejeune, J. P. (2017). Intraoperative MRI for the management of brain lesions adjacent to eloquent areas. *Neurochirurgie*. <https://doi.org/10.1016/j.neuchi.2016.12.006>
- Roberts, D. W., Hartov, A., Kennedy, F. E., Miga, M. I., & Paulsen, K. D. (1998). Intraoperative brain shift and deformation: A quantitative analysis of cortical displacement in 28 cases. *Neurosurgery*. <https://doi.org/10.1097/00006123-199810000-00010>
- Sanai, N., & Berger, M. S. (2008). Glioma extent of resection and its impact on patient outcome. In *Neurosurgery*. <https://doi.org/10.1227/01.neu.0000318159.21731.cf>
- Schonberg, T., Pianka, P., Hendler, T., Pasternak, O., & Assaf, Y. (2006). Characterization of displaced white matter by brain tumors using combined DTI and fMRI. *NeuroImage*. <https://doi.org/10.1016/j.neuroimage.2005.11.015>
- Senft, C., Bink, A., Franz, K., Vatter, H., Gasser, T., & Seifert, V. (2011). Intraoperative MRI guidance and extent of resection in glioma surgery: A randomised, controlled trial. *The Lancet Oncology*. [https://doi.org/10.1016/S1470-2045\(11\)70196-6](https://doi.org/10.1016/S1470-2045(11)70196-6)

- Shim, K. W., Park, E. K., Kim, D. S., & Choi, J. U. (2017). Neuroendoscopy: Current and future perspectives. In *Journal of Korean Neurosurgical Society* (Vol. 60, Issue 3). <https://doi.org/10.3340/jkns.2017.0202.006>
- Stummer, W., Stocker, S., Wagner, S., Stepp, H., Fritsch, C., Goetz, C., Goetz, A. E., Kiefmann, R., & Reulen, H. J. (1998). Intraoperative detection of malignant gliomas by 5-aminolevulinic acid- induced porphyrin fluorescence. *Neurosurgery*. <https://doi.org/10.1097/00006123-199803000-00017>
- Takhounts, E. G., Crandall, J. R., & Darvish, K. (2003). On the Importance of Nonlinearity of Brain Tissue under Large Deformations. *SAE Technical Papers*. <https://doi.org/10.4271/2003-22-0005>
- Taniguchi, H., Muragaki, Y., Iseki, H., Nakamura, R., & Taira, T. (2006). New radiofrequency coil integrated with a stereotactic frame for intraoperative MRI-controlled stereotactically guided brain surgery. *Stereotactic and Functional Neurosurgery*. <https://doi.org/10.1159/000094845>
- Taniguchi, M., Cedzich, C., Taniguchi, M., Cedzich, C., & Schramm, J. (1993). Modification of cortical stimulation for motor evoked potentials under general anesthesia: Technical description. *Neurosurgery*. <https://doi.org/10.1227/00006123-199302000-00011>
- Trout, J. M., Walsh, E. J., & Fayer, R. (2002). Rotifers Ingest Giardia Cysts. *The Journal of Parasitology*. <https://doi.org/10.2307/3285557>
- Tsugu, A., Ishizaka, H., Mizokami, Y., Osada, T., Baba, T., Yoshiyama, M., Nishiyama, J., & Matsumae, M. (2011). Impact of the combination of 5-aminolevulinic acid-induced fluorescence with intraoperative magnetic resonance imaging-guided surgery for glioma. In *World Neurosurgery*. <https://doi.org/10.1016/j.wneu.2011.02.005>
- Tunnacliffe, A., & Lapinski, J. (2003). Resurrecting Van Leeuwenhoek's rotifers: A reappraisal of the role of disaccharides in anhydrobiosis. In *Philosophical Transactions of the Royal Society B: Biological Sciences*. <https://doi.org/10.1098/rstb.2002.1214>
- Wallace, R. L. (2002). Rotifers: Exquisite metazoans. *Integrative and Comparative Biology*.
- Warfield, S. K., Haker, S. J., Talos, I. F., Kemper, C. A., Weisenfeld, N., Mewes, A. U. J., Goldberg-Zimring, D., Zou, K. H., Westin, C. F., Wells, W. M., Tempny, C. M. C., Golby, A., Black, P. M., Jolesz, F. A., & Kikinis, R. (2005). Capturing intraoperative deformations: Research experience at Brigham and Women's hospital. *Medical Image Analysis*. <https://doi.org/10.1016/j.media.2004.11.005>
- Warfield, S. K., Nabavi, A., Butz, T., Tuncali, K., Silverman, S. G., Black, P. M. L., Jolesz, F. A., & Kikinis, R. (2000). Intraoperative segmentation and nonrigid registration for image guided therapy. *Lecture Notes in Computer Science (Including Subseries Lecture Notes in Artificial Intelligence and Lecture Notes in Bioinformatics)*. https://doi.org/10.1007/978-3-540-40899-4_18
- Wen, P. Y., & Kesari, S. (2008). Malignant gliomas in adults. In *New England Journal of Medicine*. <https://doi.org/10.1056/NEJMra0708126>
- Wittek, A., Grosland, N. M., Joldes, G. R., Magnotta, V., & Miller, K. (2016). From Finite Element Meshes to Clouds of Points: A Review of Methods for Generation of Computational Biomechanics Models for Patient-Specific Applications. *Annals of Biomedical Engineering*. <https://doi.org/10.1007/s10439-015-1469-2>
- Wittek, A., Miller, K., Kikinis, R., & Warfield, S. K. (2007). Patient-specific model of brain deformation: Application to medical image registration. *Journal of Biomechanics*. <https://doi.org/10.1016/j.jbiomech.2006.02.021>

- Woodworth, G., McGirt, M. J., Samdani, A., Garonzik, I., Olivi, A., & Weingart, J. D. (2005). Accuracy of frameless and frame-based image-guided stereotactic brain biopsy in the diagnosis of glioma: Comparison of biopsy and open resection specimen. *Neurological Research*. <https://doi.org/10.1179/016164105X40057>
- Wu, J. S., Zhou, L. F., Tang, W. J., Mao, Y., Hu, J., Song, Y. Y., Hong, X. N., & Du, G. H. (2007). Clinical evaluation and follow-up outcome of diffusion tensor imaging-based functional neuronavigation: A prospective, controlled study in patients with gliomas involving pyramidal tracts. *Neurosurgery*. <https://doi.org/10.1227/01.neu.0000303189.80049.ab>
- Wygant, I. O., Zhuang, X., Yeh, D. T., Oralkan, Ö., Ergun, A. S., Karaman, M., & Khuri-Yakub, B. T. (2008). Integration of 2D CMUT arrays with front-end electronics for volumetric ultrasound imaging. *IEEE Transactions on Ultrasonics, Ferroelectrics, and Frequency Control*. <https://doi.org/10.1109/TUFFC.2008.652>
- Xu, L., Lin, Y., Han, J. C., Xi, Z. N., Shen, H., & Gao, P. Y. (2007). Magnetic resonance elastography of brain tumors: Preliminary results. *Acta Radiologica*. <https://doi.org/10.1080/02841850701199967>
- Yan, J. L., Van Der Hoorn, A., Larkin, T. J., Boonzaier, N. R., Matys, T., & Price, S. J. (2017). Extent of resection of peritumoral diffusion tensor imaging-detected abnormality as a predictor of survival in adult glioblastoma patients. In *Journal of Neurosurgery*. <https://doi.org/10.3171/2016.1.JNS152153>
- Yaniv, Z., Wilson, E., Lindisch, D., & Cleary, K. (2009). Electromagnetic tracking in the clinical environment. *Medical Physics*. <https://doi.org/10.1118/1.3075829>
- Yasargil, & MG. (1969). *Microsurgery Applied to Neurosurgery*. Georg Thieme Verlag / Academic Press.,
- Yrjänä, S. K., Tuominen, J., & Koivukangas, J. (2007). Intraoperative magnetic resonance imaging in neurosurgery. In *Acta Radiologica*. <https://doi.org/10.1080/02841850701280858>
- Zhao, L., & Jolesz, F. A. (2014). Navigation with the Integration of Device Tracking and Medical Imaging. In F.A. Jolesz (Ed.), *Intraoperative Imaging and Image-Guided Therapy* (Ed, pp. 259–276). Springer Science+Business Media. https://doi.org/10.1007/978-1-4614-7657-3_17